

## Unconventional Dynamics in Triangular Heisenberg Antiferromagnet $\text{NaCrO}_2$

A. Olariu,<sup>1</sup> P. Mendels,<sup>1</sup> F. Bert,<sup>1</sup> B. G. Ueland,<sup>2</sup> P. Schiffer,<sup>2</sup> R. F. Berger,<sup>3</sup> and R. J. Cava<sup>3</sup>

<sup>1</sup>*Laboratoire de Physique des Solides, UMR 8502 CNRS, Université Paris-Sud, 91405 Orsay, France*

<sup>2</sup>*Department of Physics, Pennsylvania State University, University Park, Pennsylvania 16802, USA*

<sup>3</sup>*Department of Chemistry, Princeton University, Princeton, New Jersey 08540, USA*

(Received 27 March 2006; published 18 October 2006)

We report magnetization, specific heat, muon spin rotation, and Na NMR measurements on the  $S = 3/2$  rhombohedrally stacked Heisenberg antiferromagnet  $\text{NaCrO}_2$ . This compound appears to be a good candidate for the study of isotropic triangular Heisenberg antiferromagnets with very weak interlayer coupling. While specific heat and magnetization measurements indicate the onset of a transition in the range  $T_c \sim 40\text{--}50$  K, both muon spin rotation and NMR reveal a fluctuating crossover regime extending well below  $T_c$ , with a peak of relaxation rate  $T_1^{-1}$  around  $T \approx 25$  K. This novel finding is discussed within the context of excitations in the triangular Heisenberg antiferromagnets.

DOI: [10.1103/PhysRevLett.97.167203](https://doi.org/10.1103/PhysRevLett.97.167203)

PACS numbers: 75.40.Cx, 76.60.-k, 76.75.+i

Since the initial proposal by Anderson for a liquidlike resonating valence bond state in triangular  $S = 1/2$  antiferromagnets (AF) [1], a huge number of novel states have been unveiled in triangle-based lattices. The frustration generated by the geometry of the lattice is responsible for specific low-energy excitations, which contribute to destabilization of any possible magnetic ordering. In the past decade, the fluctuating character at very low temperatures has become a prominent feature of experimental realizations of corner sharing, e.g., kagome or pyrochlore lattices. By contrast, earlier studies on edge-sharing stacked triangular AF displayed spin ordering with remarkable  $H$ - $T$  phase diagrams, and the issue of new universality classes was addressed [2]. There are strong indications that the concept of chirality, i.e., the way the spins are rotated in a  $120^\circ$  Néel order for a given triangle, might be important with, possibly, an original set of low-energy excitations [3]. Notably, the systems which have received the most attention consist of anisotropic spins [2], and the canonical Heisenberg case with isotropic interactions has not been a subject of many experimental studies.

The field of triangular Heisenberg antiferromagnets was revived quite recently by both the unpredicted discovery of superconductivity in the stacked triangular Na cobaltates family  $\text{Na}_x\text{CoO}_2$  and the spin liquidlike behavior observed in triangular compounds down to very low  $T$  [4–6]. In  $\text{Na}_x\text{CoO}_2$ , a very rich phase diagram was discovered, which may combine many possibly competing parameters such as charge order, magnetic frustration, and strong electronic correlations. In this context, the isostructural insulating magnetic compound  $\text{NaCrO}_2$  ( $S = 3/2$ ) appears to be an ideal candidate to study the effects of frustration in isolation [7]. The well separated  $\text{Cr}^{3+}$  planes stack in a strict rhombohedral  $R\bar{3}m$   $ABCABC$  structure, implying a single value of the in-plane Cr-Cr exchange constant. In the very limited data available on this compound, the maximum of the magnetic susceptibility  $\chi$  was taken as an indication of a transition around 49 K [8], and early neu-

tron scattering work [9] demonstrated a 2D character to the magnetic correlations. EPR measurements [10,11] yield a relative  $g$  anisotropy of 0.25% and point to a small single-ion uniaxial  $c$  anisotropy  $\lesssim 1$  K, therefore a dominant Heisenberg character. Finally, data on the more studied  $\text{LiCrO}_2$  member of this family [8,11,12] have revealed  $120^\circ$  spin ordering in a plane containing the  $c$  axis, which was tentatively attributed to a small easy-axis anisotropy.

In this Letter, we present the first detailed local study of  $\text{NaCrO}_2$ . Through NMR and muon spin rotation ( $\mu\text{SR}$ ), we have both investigated the static magnetic properties and revealed the existence of an intermediate dynamical fluctuating regime well below 40 K, a behavior which has not been previously observed in studies of triangular Heisenberg antiferromagnets (THAFs).

Polycrystalline  $\text{NaCrO}_2$  was prepared by mixing high purity  $\text{Na}_2\text{CO}_3$  and  $\text{Cr}_2\text{O}_3$ , with 2% Na in excess of the stoichiometric amount, and grinding in an agate mortar. The mixture was pressed into pellets, wrapped in Zr foil, and heated in a dense alumina boat at  $T = 750^\circ\text{C}$  for 30 h under flowing Ar, with one intermediate grinding. Characterization of the samples by powder x-ray diffraction showed them to be single phase with excellent crystalline quality.

dc magnetic susceptibility measurements performed in the  $T = 5\text{--}300$  K range (Fig. 1) are in perfect agreement with an earlier study up to  $T = 800$  K and yield  $\Theta_{\text{CW}} \sim 290$  K and  $\mu_{\text{eff}} = 3.78\mu_B$  [8]. Previous work suggested that the in-plane antiferromagnetic exchange  $J \sim 20$  K was due mainly to direct exchange through the overlap of nearest neighbor  $\text{Cr}^{3+}$  orbitals [13]. We have found that  $\chi$  continuously increases down to  $T = 49$  K, where a broad maximum is observed. From a comparison with samples having Ga substituted for Cr, the low- $T$  increase of  $\chi$  can be attributed to less than 1% spinless defects.

We also measured specific heat using a Quantum Design PPMS system. Measurements on the isostructural, non-magnetic compound  $\text{NaScO}_2$  were scaled and used to

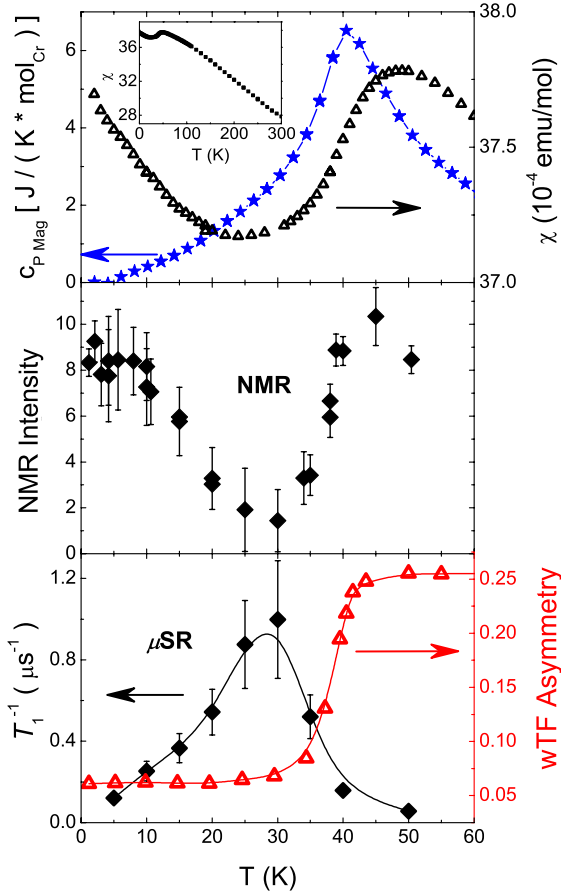


FIG. 1 (color online). Top: Magnetic specific heat (left axis) and magnetic susceptibility (right axis) versus temperature. Inset:  $\chi(T)$  on an expanded  $T$  range. Middle panel: Evolution of the NMR intensity with  $T$ . Bottom:  $\mu$ SR, left:  $T$  variation of  $T_1^{-1}$ , right: weak transverse field  $\mu$ SR asymmetry (see text).

subtract out lattice contributions. The resulting magnetic specific heat is displayed in Fig. 1. The peak at  $T_c = 41$  K is much broader than would be expected for a long range ordering transition.

Na NMR measurements were carried out in the range  $T = 1.2$ –300 K. The  $^{23}\text{Na}$  nucleus ( $\gamma/2\pi = 11.2618$  MHz/T) has a spin  $I = 3/2$  and is located in between the center of two Cr triangles from adjacent layers. Above  $T = 80$  K, the spectra were obtained by combining spin echo Fourier transforms taken at various frequencies in a  $H = 7$  T fixed field. Below  $T = 80$  K, the spectra were recorded by sweeping the magnetic field in the  $H = 6$ –7 T range at a fixed frequency of 74.527 MHz.

We first focus on the  $-1/2 \rightarrow 1/2$  transition in the paramagnetic regime (Fig. 2, inset). The line shift hardly varies (maximum 0.007%) between  $T = 80$ –300 K, whereas a sizeable linewidth of approximately 0.1%, slightly varying with temperature, is observed. The hyperfine contribution to the coupling between Cr and Na (mediated by the oxygen) is therefore very weak and dominated by the  $\text{Cr}^{3+}$ -Na dipolar interaction. This is quantitatively confirmed by our dipolar simulations, which

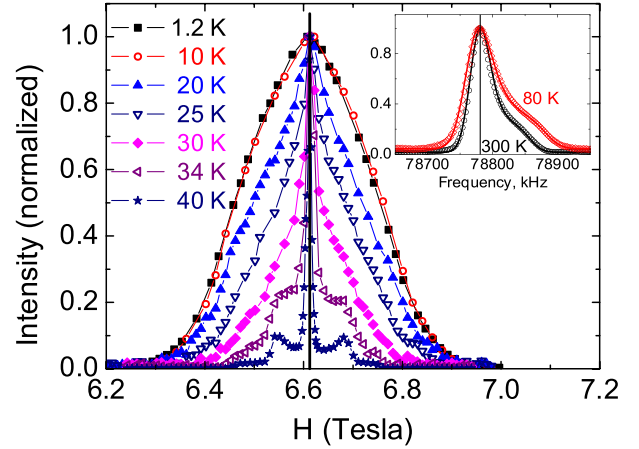


FIG. 2 (color online).  $^{23}\text{Na}$  NMR spectra for  $T < 80$  K. The vertical bar represents the unshifted reference field. The spectra have been normalized to the maximum intensity. First order quadrupolar singularities are clearly observed at 40 K for  $H = 6.54$  and 6.68 T. Inset: Fourier transform spectra at 80 and 300 K with dipolar fits (continuous lines, see text).

account for the observed asymmetric line shape (see Fig. 2, inset), and agrees within 20% with the  $\text{Cr}^{3+}$  magnetic moment extracted from our SQUID measurements. As a comparison, the hyperfine coupling is here 70 times smaller than in  $\text{Na}_{0.7}\text{CoO}_2$ . Since Na-O paths are only slightly different between these compounds, we can attribute the smallness of the Na-O-Cr hyperfine coupling to a negligible overlap of O with Cr, which is expected from the more ionic character of Cr. Hence, we can safely infer that (i) the intralayer Cr-O-Cr coupling is dominated by *direct* Cr-Cr exchange, which confirms Ref. [13], and (ii) the exchange between Cr in different layers is negligible. Therefore, the interlayer Cr-Cr coupling is found to be of a dipolar nature and, thus, very weak ( $\sim 0.01$  K). This indicates that  $\text{NaCrO}_2$  is an excellent experimental realization of a THAF.

We now describe the low- $T$  NMR local study of the frozen state (Fig. 2). In the case of a conventional magnetic transition at  $T_c = 41$  K, one would expect a growth of the internal field, i.e., the order parameter, within a few K below  $T_c$ . Because of powder averaging, this should translate into a drastic broadening of the NMR spectrum. Strikingly, we find that the broadening is evident only below 30 K, much lower than  $T_c$ . As an illustration, one can still distinguish the first order quadrupolar singularities above 30 K, and only a negligible broadening of the central line occurs for  $30 < T < 40$  K. At lower  $T$ , the linewidth at half maximum of the central line is found to saturate below 10 K (Fig. 3).

Because of powder averaging, each Na site inequivalent with respect to the magnetic structure will contribute to the line shape through a rectangular pattern, the width of which is twice the internal field  $H_{\text{int}}$ . In a simple conventional  $120^\circ$  three-lattice Néel state, a given Cr plane yields two sets of Na sites, associated with the alternating  $\pm$  chirality

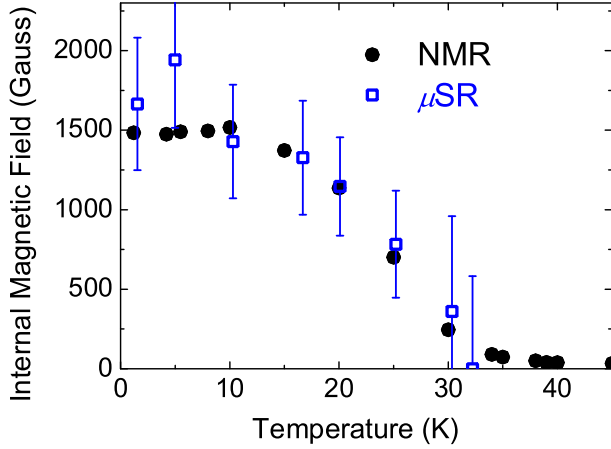


FIG. 3 (color online).  $T$  evolution of the internal field measured at the site of the *detected* nuclei or of the muon (see text).

of adjacent Cr triangles. The number of overall inequivalent sites and, thus, the distribution of  $H_{\text{int}}$  depend drastically on the type of stacking along the  $c$  axis. In addition, dipolar field values strongly depend on the orientations of the moments. Therefore, it was found to be unfeasible to simply discriminate from the low- $T$  dome-shaped line between various plausible ordered structures [9,12]. It is also not possible to distinguish between a disordered freezing and a quite complex ordered state. In any case, the low- $T$  saturation value of 1500 G determined from the linewidth is consistent with a simple estimate of the dipolar field using one nearby plane only. A precise knowledge of the magnetic structure would be necessary for any further quantitative discussion.

The major finding from our NMR study lies in the wipeout of the NMR integrated intensity (Fig. 1), i.e., the number of detected nuclei [14]. The loss of intensity results from a distribution of relaxation times, a large part of which becomes shorter than the  $\sim 10 \mu\text{s}$  lower limit of the NMR time window [15–17]. In conventional transitions, the wipeout of the signal occurs over a very narrow  $T$  range around the transition and is related to the slowing down of fluctuations from the paramagnetic to the static state. Here the full intensity is only recovered below 10 K, indicating a 30 K-broad regime of slow fluctuations. Also, the minimum intensity, i.e., the maximum of relaxation, is around  $T = 25(5)$  K, at least 25% lower than  $T_c$  where the first signs of freezing are observed. This original *intermediate extended fluctuating regime* is most likely related to the frustrated triangular network of  $\text{NaCrO}_2$ .

In order to get more insight into this dynamical regime, we performed complementary  $\mu\text{SR}$  experiments at PSI (Switzerland) and ISIS (UK) facilities. The  $\mu\text{SR}$  time window (10 ns–15  $\mu\text{s}$ ) is much better suited to tracking the persisting dynamics in slowly fluctuating magnets. In addition,  $\mu\text{SR}$  allows us to probe *all* sites, whereas only a weak fraction of the sites were detected in NMR between 20 and 40 K. Fully polarized implanted  $\mu^+$  (gyromagnetic ratio  $\gamma_\mu/2\pi = 135.5 \text{ MHz/T}$ ) interact through dipolar

coupling with the local magnetic environment. As commonly assumed in oxides, muons most probably stop  $\sim 1 \text{ \AA}$  away from  $\text{O}^{2-}$  sites.

Weak transverse field (20 G) experiments were performed to track the spin freezing, since only muons close to paramagnetic (unfrozen) sites should oscillate around the applied field direction. Figure 1 shows a drastic loss of asymmetry below 40 K, which indicates a freezing corresponding to the specific heat maximum.

Zero field asymmetry curves are presented in Fig. 4. Above  $T_c$ , in the fast fluctuation regime, muons mainly sense a weak magnetic field due to  $\sim 2 \text{ G}$  static nuclear dipoles. The decrease of the  $\mu^+$  polarization had the expected Kubo-Toyabe shape, Gaussian at early times, whereas electronic spin fluctuations result in very modest relaxation with  $T_1^{-1} \sim 0.06 \mu\text{s}^{-1}$  [18].

Below the transition temperature, we expect the asymmetry to evolve with time according to:

$$A = A_0 \left[ \frac{2}{3} \cos(2\pi\nu t + \phi) e^{-\lambda t} + \frac{1}{3} \right] e^{-(t/T_1)^\alpha} + B. \quad (1)$$

The constant  $A_0$ , of the order of 0.25, stands for the maximum asymmetry at 100% beam polarization, and  $B$  arises from muons not stopping inside the sample. The oscillating term corresponds to the  $\mu^+$  precession around the internal magnetic field ( $H_\mu$ ) direction at the average frequency  $\nu = \gamma_\mu H_\mu$ , while the damping of the oscillation is due to the width of the internal field distribution  $\lambda/\gamma_\mu$ . In the case of static behavior, we obtained the so-called “one-third tail” at long times,  $A \rightarrow A_0/3 + B$ , since we expect  $T_1^{-1}$  to be negligibly small. In general, dynamical processes can be clearly singled out at long times on the relaxation of this one-third tail, which enables one to keep track of the evolution of  $T_1^{-1}$  with  $T$ .

A high statistics run taken at  $T = 5 \text{ K}$  is displayed in the inset in Fig. 4. The early time oscillating behavior is made

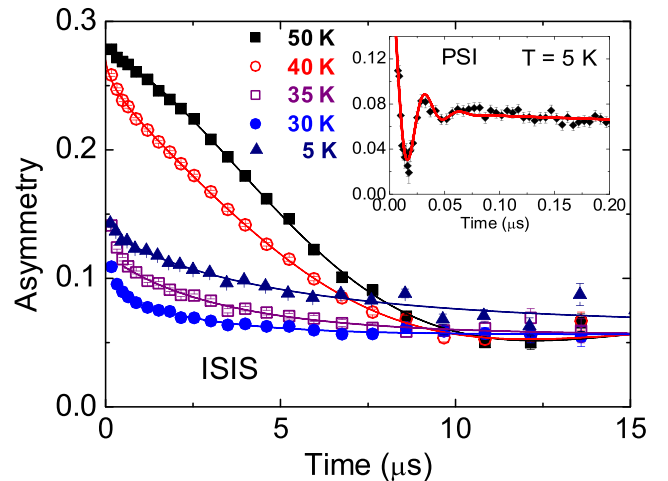


FIG. 4 (color online). Main panel (ISIS):  $\mu\text{SR}$  asymmetry in zero external field. Inset (PSI): Early time asymmetry at  $T = 5 \text{ K}$ . The background is different for the two setups. Lines are for fits.

clear by the two visible wiggles and rules out a completely disordered picture. A  $H_\mu \sim 1900$  G internal field is estimated from the  $\nu = 26$  MHz frequency of the oscillations. The fast early time damping indicates a large 1600 G distribution of  $H_\mu$ , maybe related to sizable disorder. The weakness of relaxation indicates a purely static magnetic frozen phase in the low- $T$  limit.

At higher  $T$ , the internal field is found to decrease and cannot be followed any more above 32 K (Fig. 3). The order of magnitude of the internal field agrees very well with our NMR findings, issued in both cases from dipolar coupling of the probe to its surrounding.

We now focus on the relaxation effects evidenced on the  $t > 0.1 \mu\text{s}$  one-third tail displayed in the main frame in Fig. 4. The increase of relaxation between 5 and 30 K is clearly visible,  $T_1^{-1}(30 \text{ K}) \sim 1 \mu\text{s}^{-1}$ , followed by a decrease at  $T = 35$  K (Fig. 1, bottom). A broad maximum of the relaxation rate is found to occur around 25–30 K [19]. This peak was found to be progressively washed out in samples having Ga substituted for Cr, which demonstrated its intrinsic character.

To summarize, our specific heat, susceptibility, NMR wipeout, and  $\mu\text{SR}$  data point to an *onset* of gradual freezing at  $T_c \approx 41$  K, associated with a slowing down of spin fluctuations. Below this temperature, a crossover regime occurs, marked by a maximum in the relaxation rate at  $0.75T_c$ . This broad fluctuating regime extends down to  $0.25T_c$ . Neither a conventional transition at 41 K nor around 30 K can simply reconcile these findings.

One possibility is that the  $T_1^{-1}$  peak signals a subsequent transition. To our knowledge, the splitting of the transition temperature has been observed only in a very narrow temperature range ( $< 3$  K) for triangular AF, e.g., the quasi-2D  $VX_2$  ( $X = \text{Cl, Br, I}$ ) and the quasi-1D  $ABX_3$  systems [2], both with single-ion anisotropy. The scenario of a second magnetic transition at  $T = 30$  K can be safely ruled out here in view of the weak anisotropy, which contrasts with the large temperature range between  $T_c$  and the  $T_1^{-1}$  maximum. Also, no sign of a second peak is detected in the specific heat, and, finally, the broad fluctuating regime points to a dynamical crossover between states rather than a sharp transition. Whatever the transition scenario, our study definitely reveals novel excitations. Such a specific feature of the isotropic THAF was clearly pointed out by recent calculations [20,21].

One can speculate that the dynamical regime could be evidence for topological “ $Z_2$ ” excitations in the chirality vortex regime [3]. The latter can be viewed as the pendant of excitations for the  $XY$  spins, well known to drive the Kosterlitz-Thouless transition. The 30 K temperature could then be the equivalent of that transition, i.e., resulting from the coupling between the  $Z_2$  vortex and antivortex. Interestingly, the existence of  $Z_2$  vortices has been suggested above  $T_c$  to interpret EPR data in  $\text{LiCrO}_2$  and  $\text{VX}_2$  [22,23] and for the spin liquid state found in  $\text{NiGa}_2\text{S}_4$  [4].

Whether the spin texture of the ground state can be singled out is a matter for future research.

Regardless of interpretation, with its 2D Heisenberg character,  $\text{NaCrO}_2$  together with recent systems [4–6] form a bridge between two intensively studied classes of systems. On one side, corner sharing Heisenberg AF, characterized by a fluctuating regime extending down to very low  $T$  and marginal orders, e.g., the kagome-based compounds [16,24,25]. On the other side, the case of anisotropic triangular AF, which order at low  $T$  with two successive transitions in a narrow  $T$  range. Our data strongly support renewed study of the  $\text{ACrO}_2$  family including local measurements of the  $A = \text{Li, K}$  compounds and modern neutron studies of the entire family.

We thank H. Alloul, J. Bobroff, O. Cépas, M. Elhajal, G. Lang, L. Lévy, C. Lhuillier, and P. Viot for fruitful discussions and A. D. Hillier and A. Amato for assistance at  $\mu\text{SR}$  facilities. This work was supported by the European Commission EC FP6 grants. We gratefully acknowledge support from NSF Grant No. DMR-0353610, CNRS-NSF, and I2CAM (B. U.).

- 
- [1] P. W. Anderson, Mater. Res. Bull. **8**, 153 (1973).
  - [2] M. F. Collins and O. A. Petrenko, Can. J. Phys. **75**, 605 (1997).
  - [3] H. Kawamura, J. Phys. Condens. Matter **10**, 4707 (1998).
  - [4] S. Nakatsuji *et al.*, Science **309**, 1697 (2005).
  - [5] Y. Shimizu *et al.*, Phys. Rev. Lett. **91**, 107001 (2003).
  - [6] R. Coldea *et al.*, Phys. Rev. Lett. **86**, 1335 (2001).
  - [7] In the parent  $\text{NaCoO}_2$  compound,  $\text{Co}^{3+}$  is nonmagnetic.
  - [8] C. Delmas *et al.*, J. Phys. Chem. Solids **39**, 55 (1978).
  - [9] J. L. Soubeyroux *et al.*, J. Magn. Magn. Mater. **14**, 159 (1979).
  - [10] P. R. Elliston *et al.*, J. Phys. Chem. Solids **36**, 877 (1975).
  - [11] S. Angelov *et al.*, Solid State Commun. **50**, 345 (1984).
  - [12] H. Kadowaki, H. Takei, and K. Motoya, J. Phys. Condens. Matter **7**, 6869 (1995).
  - [13] K. Motida and S. Miyahara, J. Phys. Soc. Jpn. **28**, 1188 (1970).
  - [14] In our experiment, we use a conventional  $\pi/2$ - $\tau$ - $\pi$  pulse sequence. The detected signal was extrapolated to  $\tau \rightarrow 0$  to calculate the intensity and corrected for  $T$  effects.
  - [15] A. W. Hunt *et al.*, Phys. Rev. Lett. **82**, 4300 (1999).
  - [16] P. Mendels *et al.*, Phys. Rev. Lett. **85**, 3496 (2000).
  - [17] D. E. MacLaughlin and H. Alloul, Phys. Rev. Lett. **36**, 1158 (1976).
  - [18] Early times on high- $T$  spectra (not shown) reveal about 5% spurious magnetic phase.
  - [19] Note that the value of the stretched exponent  $\alpha \sim 0.5$  indicates a distribution either of  $T_1$  or of muon sites.
  - [20] W. Zheng *et al.*, Phys. Rev. Lett. **96**, 057201 (2006).
  - [21] S. Fujimoto, Phys. Rev. B **73**, 184401 (2006).
  - [22] Y. Ajiro *et al.*, J. Phys. Soc. Jpn. **57**, 2268 (1988).
  - [23] N. Kojima *et al.*, J. Phys. Soc. Jpn. **62**, 4137 (1993).
  - [24] D. Bono *et al.*, Phys. Rev. Lett. **92**, 217202 (2004).
  - [25] F. Bert *et al.*, Phys. Rev. Lett. **95**, 087203 (2005).